Microelectronics Reliability 51 (2011) 1264–1270

Contents lists available at ScienceDirect

Microelectronics Reliability

journal homepage: www.elsevier.com/locate/microrel

Noise properties of thick-film resistors in extended temperature range

Adam Witold Stadler *

Department of Electronics Fundamentals, Rzeszow University of Technology, W. Pola 2, 35-959 Rzeszow, Poland

ARTICLE INFO

Article history:
Received 13 December 2010
Received in revised form 9 February 2011
Accepted 25 February 2011
Available online 31 March 2011

ABSTRACT

Results of thorough experimental studies on electrical properties of thick-film resistors (TFRs) have been overviewed and summarized. Experiments covered resistance and noise measurements in wide temperature range. Low-frequency noise spectroscopy has been used for the investigations of fluctuating phenomena. Sample resistors were prepared of various combinations of commercial and laboratory-made conducting and resistive pastes and printed on alumina substrates. Resistive pastes were made of materials: (i) Pb-containing RuO_2- and $Bi_2Ru_2O_7$-based, (ii) Pb/Cd-free RuO_2-, $CaRuO_3$-, and $RuO_2/CaRuO_3$-based. Conducting pastes included Ag, Ag–Pd and Ag–AgPt–Pd, Au, PtAu as a main ingredients. Electrical properties of various TFRs made of different materials were compared. Cross-correlation technique of noise spectra measurements in conjunction with the multiterminal configuration of TFRs was used in investigations of noise vs. resistor volume, resulting in extraction of noise components originated in different parts of the resistor. Furthermore, noise of the resistor was split up into bulk and interface noise. Resistance noise, observed in all studied TFRs, has been found to consist of background $1/f$ noise and Lorentzian noise induced by thermally activated noise sources (TANSs). Properties of TANSs have been described and their relation to TFRs performance parameters have been pointed out. Noise properties of various Pb-containing and Pb/Cd-free resistive materials have been compared with the use of bulk noise intensity parameter, C_{bulk}. Conclusions concerning compatibility of resistive and conductive pastes have been formulated. They might be useful in further improvement of materials systems for thick-film technology in order to fabricate low-noise and stable passives.

1. Introduction

Thick-film resistors (TFRs) have been widely used in microelectronics for many years. Offering wide range of sheet resistances, they are used as passives in commercial temperature range due to their excellent performance parameters, like small value of temperature coefficient of resistance (TCR), good linearity, and good power dissipation ability. On the other hand, RuO_2-based TFRs offer very high resistance sensitivity to temperature and good reproducibility in low temperatures [1–3]. Hence, they enter the field of resistance temperature sensors for cryogenics, being resistant to magnetic field and radiation, what is of fundamental importance in certain kind of experiments. All above advantages are available by the use of relatively simple and cheap technology.

During many years of evolution, TFRs achieve satisfactory noise level, which relates to electronic devices and circuits reliability. However, new fields of applications reveal new phenomena that take place in these TFRs. For example, it has been found, that noise intensity in TFRs of RuO_2 rapidly rises when temperature drops below a few Kelvin [4], significantly degrading temperature resolution of the sensor [5]. The reason for such behaviour is unclear as the electrical transport mechanism in TFRs is still the matter of argument. Most often there were considered such mechanisms like thermally activated tunneling [6], fluctuation induced tunneling [7–9], conduction in a narrow band [10], variable range hopping (VRH) [11,12], space charge limited transport [13], emissions over graded barriers [8], and weak localization [14].

Conventionally TFRs are manufactured as resistive films of several tens μm thickness spanned between conducting terminations/contacts, by deposition of resistive and conducting inks on proper substrates. The resistive pastes consist of conducting metallic oxides (mainly RuO_2), insulating glass (typically lead-borosilicate) while conducting pastes base on metals (Au, Ag, Pd) or their compounds and/or mixtures. Both pastes include an organic vehicle to gain necessary rheological properties. Manufacturers add also additions (modifiers and stabilizers). Present law regulations force microelectronics to switch to Cd/Pb-free materials, opening new field of exploration. Solders and pastes for thick-film technology have to be replaced by their Cd/Pb-free counterparts. However, new materials are far from maturity and have to be significantly improved in order to fabricate low-noise, stable and reliable TFRs.

In this work, studies of electrical properties of TFRs, made of Pb-containing and Cd/Pb-free materials, that base on low-frequency noise measurements are presented. Apart from identification of noise and its components, also other fluctuating phenomena were

* Tel.: +48 178651116.
E-mail address: astadler@prz.edu.pl

0026-2714/$ - see front matter © 2011 Elsevier Ltd. All rights reserved.
doi:10.1016/j.microrel.2011.02.023

detected and have been analyzed. This analysis relay mostly on the so called "noise maps", which show the evolution of the noise spectra with changing the temperature and have been obtained by the use of low-frequency noise spectroscopy (LFNS) in wide temperature range.

2. Samples preparation

2.1. Materials

TFRs made of various combinations of commercial and lab-made resistive and conductive pastes have been prepared in high- and low-temperature process. RuO_2, $Bi_2Ru_2O_7$, and $CaRuO_3$ materials were used as a conducting phase in resistive pastes, whereas conductive pastes based on Au, Ag, PdAg, PtAu, Ag–AgPt–Pd. Pb-containing commercial pastes (DuPont and ITME – Institute of Electronic Materials Technology, Warsaw, Poland) based on either RuO_2 (Du Pont) or bismuth ruthenate (ITME) while laboratory made pastes consist of RuO_2 (10% and 12% RuO_2 by volume) and lead borosilicate glass (10% B_2O_3, 15% SiO_2, 65% PbO). Contacts were made of pastes from Metech, Du Pont, Electro-Science Laboratories (ESL) and ITME, which contain Au, Pt, Pd and Ag as basic ingredients.

Pb/Cd-free TFRs have been made with the use (i) resistive pastes which include RuO_2 (35% by vol.) or $CaRuO_3$ (26.5%) or 1:1 by weight mixture of $RuO_2/CaRuO_3$ (28%) and complex glass and (ii) conductive pastes P-121 (Ag), P-220 (AgPd), and P-511 (Ag–AgPt–Pd), all from ITME.

2.2. Geometry

Multiterminal pattern of the resistive film with two opposite current terminations and several evenly spaced voltage probes has been designed. The main resistive film has $L = 15$ mm length and $w = 1$ mm width [15–18]. The sample TFR with the terminal numeration is shown in the inset of Fig. 1. Such shape of the resistor was designed to take advantages of cross-correlation technique and extract noise components originated in different parts of the device [16].

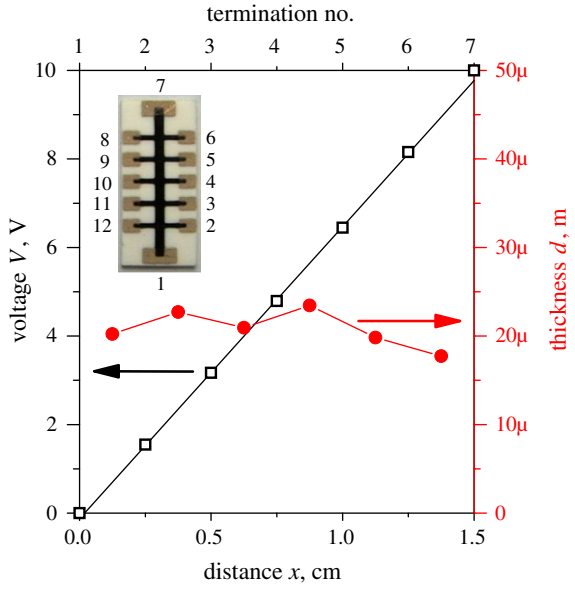

Fig. 1. Voltage (squares) and thickness (solid circles) distributions along the resistive film. The picture of the sample TFR with the terminations numbering is shown in the inset.

2.3. Printing and firing

Resistive pastes were printed onto alumina substrates through 200 mesh screen. After drying in 120 °C for 15 min, films were fired in a tunnel furnace gaining the final thickness of 20–25 µm (Fig. 1). The process of firing followed a suitable temperature profile with peak temperature at 850 °C lasting 10 min. However, for certain RuO_2-based samples also other peak temperatures were used. Contacts to the films were made of conductive pastes in a very similar process. They were deposited onto substrates prior to the resistive films printing. Apart from conventional alumina substrates sample resistors were also deposited onto low-temperature co-fired ceramic (LTCC) substrates made of DuPont green tape DP 951 [19]. In this case substrate (ceramic) and resistors were either fired together (co-fired) or separately (post-fired).

2.4. Selection

For any combination of conducting and resistive pastes, several samples were prepared. From each series a pair of samples, which match their room temperature resistance measured between terminations 1 and 7 ($R \equiv R_{1-7} = V_{1-7}/I$, where I is biasing current and V_{1-7} is the voltage between terminations 1–7), has been selected for noise studies. Preliminary tests of selected samples covered also thickness and voltage distributions measurements. The latter enables one to calculate sheet resistance and evaluate size effect, which characterize quality of the contacts. Size effect, *SE*, was defined as the ratio of the average resistance per square, $R_{1-7}w/L$, and "bulk" sheet resistance $R_{sq} = (V_6 - V_2)w/(L_{2-6}I)$, where L_{2-6} is the length of the sector of the resistive film that span between contacts 2–6 and $(V_6 - V_2)$ is the voltage across this sector. Exemplary plots of thickness and voltage distributions along the resistive layer for $RuO_2/CaRuO_3$ TFR are shown in Fig. 1.

3. Noise measurements

Advantages of dc bridge configuration shown in Fig. 2 have been taken to measure noise in the selected pairs of TFRs. Only the samples and calibrated temperature sensor (Pt-100 RTD) were inserted into either LN or LHe cryostat and subjected to cooling. The resistor R_B took the value of 1 MΩ–3 MΩ, depending on the sample resistance R_{1-7}, which always was less than 100 kΩ, to ensure the proper sample bias and sufficient damping of power supply noise as well as the noise coming from the upper part of the resistor. Using virtual instrument concept, Noise Signal Analyzer has been developed to manage the experiment [20]. It acquires voltages from bridge diagonal (V_{7-7}) and subdiagonals (V_{6-6}, V_{5-5}, V_{3-3}, V_{2-2}), and then (i) processes them by the use of ac–coupled differential low-noise amplifiers and low-pass filters, (ii) calculates voltages V_{2-6}, V_{3-5}, and V_{6-7} across sectors 2–6, 3–5, 6–7 of TFRs ($V_{x-y} = V_{y-y} - V_{x-x}$), (iii) in real-time calculates spectra of V_{7-7} as well as cross-spectra of V_{7-7} and voltages V_{6-6}, V_{2-2}, V_{2-6}, V_{3-5}, V_{6-7}. Noise (cross-)spectra were calculated as (cross-)power spectral densities (PSD) of voltage fluctuations using FFT algorithm for records of 2 s duration with 2^{19} samples. Only low-frequency part (0.5 Hz–5 kHz) of the averaged (over 600 s period) spectra were recorded continuously by the Analyzer together with additional data, like actual temperature, resistance and bias voltage. During noise spectroscopy experiments slow rise of samples temperature has been applied.

The usage of cross-correlation technique reject noise induced by voltage probes [16] and thus enable one to measure noise components originated from different sectors of TFRs. Due to the equipment limitations, only the voltages from TFRs sectors: 1–7 (whole resistor), 1–6, 2–6, 3–5, and 6–7 were acquired simultaneously.

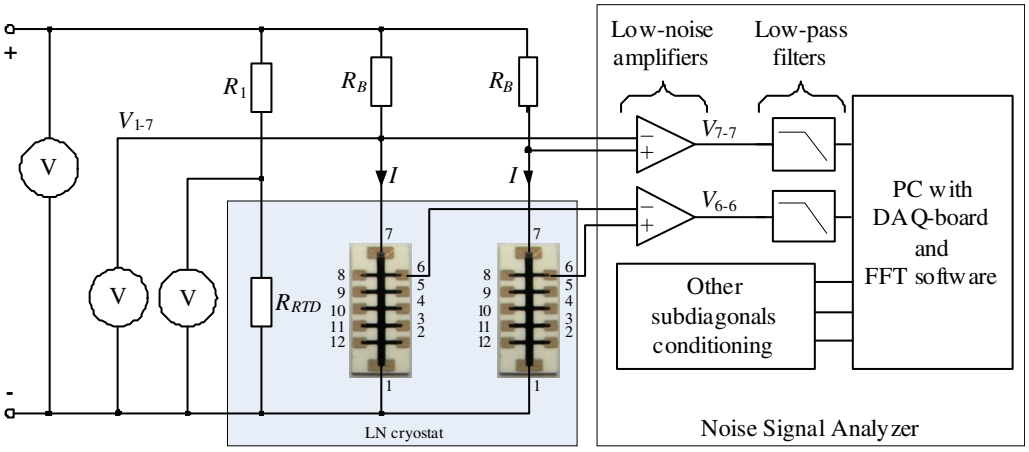

Fig. 2. dc bridge configuration for noise measurements in TFRs.

Out of these sectors, only the sectors 2–6 and 3–5 have spectra that are free from noises generated in current contacts, while spectra acquired for sectors 1–7 include noise generated in both upper and lower current contact, and spectra for sectors 1–6 (6–7) contain noise generated only in lower (upper) current contact. Noise spectra and cross-spectra, were measured for non-zero bias (S_V) as well as for zero bias ($S_{V=0}$) to calculate excess noise, $S_{Vex} = S_V - S_{V=0}$.

4. Experiment

4.1. Temperature dependence of resistance

Typical temperature dependence of resistance, $R(T)$, measured on terminations 1–7 in temperature range from 1 K to 300 K, has been shown in Fig. 3. Additionally, temperature coefficient of resistance and dimensionless sensitivity, $A \equiv (T/R)|dR/dT|$ (dashed lines), have been calculated and plotted in the inset of Fig. 3. Depending on the TFRs, $R(T)$ is either monotonic or has one minimum. For all TFRs, $R(T)$ curves are smooth and have negative TCR in low temperatures. Relatively large sensitivity for RuO_2-based TFRs confirms their usefulness in temperature sensing.

4.2. Noise sources

Two excess noise components have been found in noise spectra: (i) $1/f$ noise and (ii) Lorentzian noise generated by two-state systems. Exemplary plots of the product of excess noise S_{Vex} and frequency f vs. frequency measured at room temperature for RuO_2/$CaRuO_3$ TFRs with different contacts are shown in Fig. 4. Noise intensity can be defined as the product fS_{Vex} averaged over certain frequency band. In the inset of Fig. 4, plots of noise intensity vs. sample bias voltage, for sample P-511, are shown. Both noise components depend linearly on sample voltage square, what means that they originate from resistance fluctuations [16–18]. However, sublinear dependence has been also observed in temperature below 1 K in RuO_2-based TFRs [4], where the noise was suppressed by the excitation voltage due to the inhomogeneous self-heating

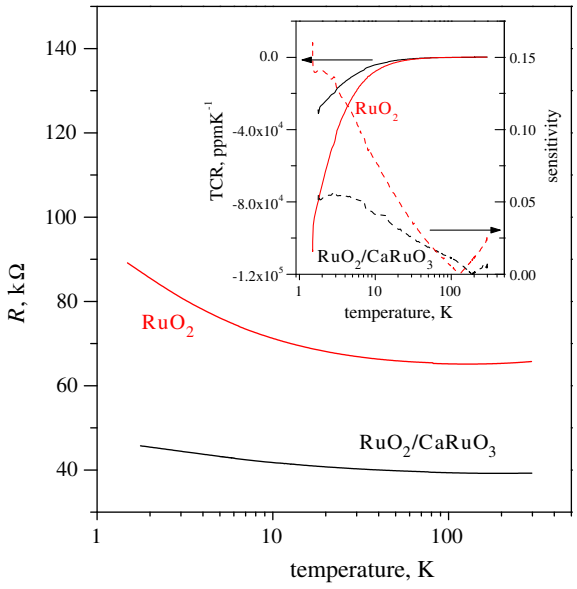

Fig. 3. Temperature dependence of resistance of Pb/Cd-free TFRs. Their TCR and sensitivity have been shown in the inset.

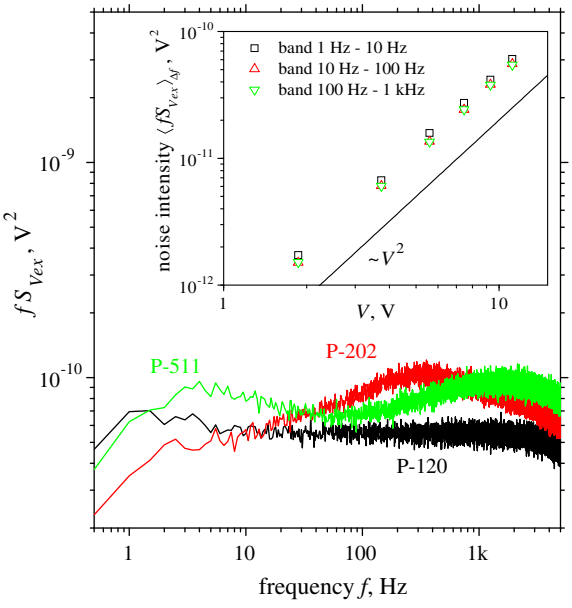

Fig. 4. Product of excess noise and frequency for Pb/Cd-free TFRs (with different contacts given in the labels denoted spectra) plotted vs. frequency. In the inset: noise intensity in different frequency bands vs. sample bias voltage, calculated for sample P-511.

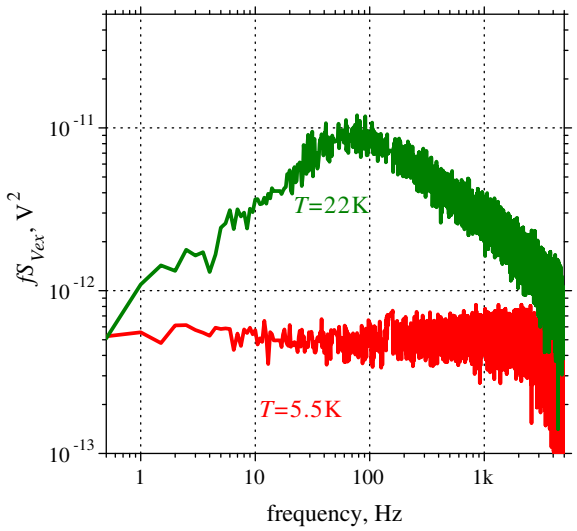

Fig. 5. Excess noise spectra for $RuO_2/CaRuO_3$ TFR with contacts made of P-511 paste.

[21]. Fluctuating mobility is supposed to be a physical mechanism that is responsible for resistance fluctuations in TFRs [4]. Lorentzians contribute to noise also in low temperatures, what is shown in Fig. 5 (data series for $T = 22$ K). However, at $T = 5.5$ K only pure $1/f$ noise was observed.

Since PSD of resistance fluctuations ($S_R = S_{Vex}/I^2$) is bias independent, it has been used in noise maps. The latter are contour graphs of the product fS_R plotted vs. frequency and reciprocal temperature $1/T$, prepared to illustrate spectra evolution in temperature [4] [16–18]. In such graphs, thermally activated noise sources (TANSs) are visible as streaks whereas smooth surface between them refers to pure $1/f$ noise. Typical noise maps prepared for low temperature range have been shown in Fig. 6a and b. Fig. 6a and b concern spectra measured for Pb/Cd-free $RuO_2/CaRuO_3$ TFR with contacts made of paste P-511 on terminations 1–7 and 6–7, respectively. Two TANSs are visible in the plot of Fig. 6a. They differ in activation energy and corresponding noise intensity they generate. One of the TANSs from Fig. 6a is also visible in Fig. 6b. Hence, this TANS is located somewhere in sectors 6–7, while the other TANS from Fig. 6a is located outside this sector.

5. Discussion

5.1. Properties of thermally activated noise sources

In all studied TFRs Lorentzians were visible on noise maps in temperatures above 15 K [15–18]. On the other hand, it has been experimentally observed that relative noise in TFRs of RuO_2 rises sharply when temperature drops below ~10 K [4]. Furthermore, it has been shown, in the framework of Dutta, Dimon and Horn (DDH) theory, that at $T \approx 10$ K there is a change of mechanism coupling microscopic noise to resistance [4]. In higher temperature this mechanism is temperature independent, e.g. noise sources could modulate rates of tunneling transitions, most probably via modulation of barrier heights for thermally activated tunneling transitions in the conduction path. Below 10 K temperature dependent coupling mechanism results in power-law dependence of microscopic noise on temperature with exponent −2 (e.g. noise sources could modulate energies of thermally activated processes).

TANSs were observed in all but LTCC TFRs [15]. They are responsible for excess noise and are associated with two-state systems. The existence of two-states systems in a glassy matrix of thick resistive films was postulated to explain resistance relaxation observed in carbon and RuO_2 thick-film low-temperature thermometers [22]. Moreover, for $T > 10$ K experimental data presented on noise maps are in line with DDH theory [4], which assumes that thermally activated transitions occur between the states of approximately equal energy, which are unlikely in a pure bulk crystal in thermal equilibrium [23]. Hence, it is most probably that the noise is generated by random two-state thermally activated transitions that take place in grain boundaries and/or localized energy states in the glass. They couple to local resistances. As in these types of materials (metal–insulator mixture) current flow is highly inhomogeneous, only those TANSs that modulate critical resistances in the percolation path are visible on the maps [16]. The latter are sample-, rather than material-dependent because different TANSs modulate critical resistances in samples. The activation energy, E_a, of TANSs detected on noise maps and appropriate attempt time τ_0 could be calculated from the approximation of the streaks visible on noise maps with the line $f = (\pi\tau_0)^{-1}\exp(-E_a/kT)$, where k is Boltzmann constant [18], e.g. on the map in Fig. 6a TANSs of activation energies 33 meV and 40 meV are visible. Activation energies found for other TFRs [15–18] range between 0.0145 eV and 0.74 eV, while τ_0 is in the range 0.12–127 ps. Our values of activation energy are a bit lower than the value $E_a = 1.52$ eV found in [24] for IrO_2 films, however

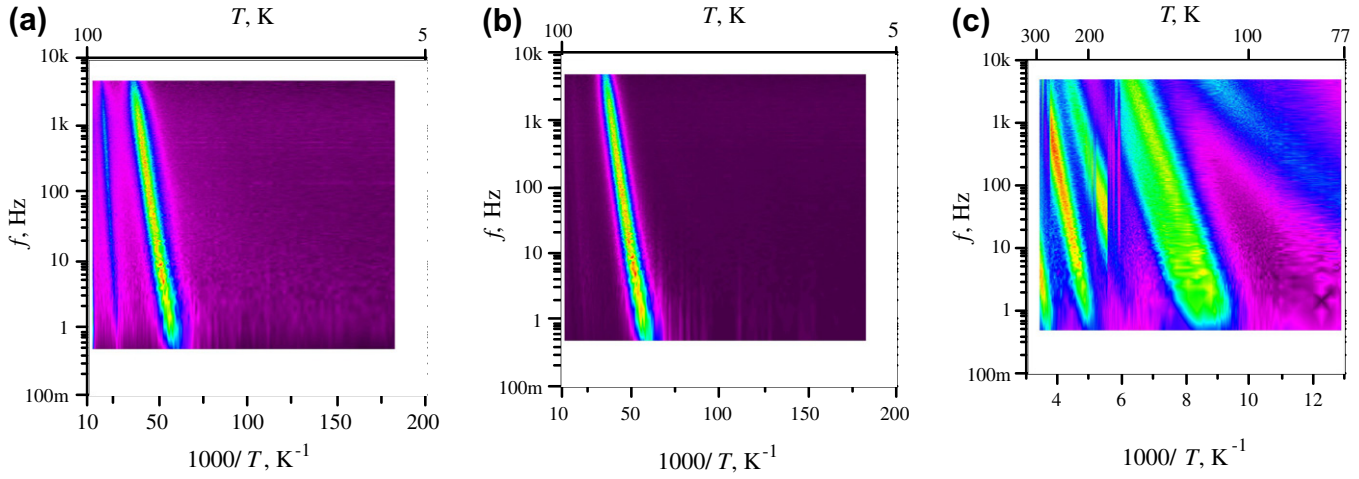

Fig. 6. Noise maps for Pb/Cd-free $RuO_2/CaRuO_3$ TFR measured on terminations 1–7 (a) and 6–7 (b) and (c).

different TANSs are active in the experiment that covered temperature range up to 800 K.

Careful examination of noise maps gathered for examined samples [15–18] allow evaluating further features of TANSs in TFRs:

- TANSs are non-uniformly distributed within the resistive film (see Fig. 6a and b).
- TANSs that are localized in sectors of TFR adjacent to current contacts are non-stationary [18]. Density and/or intensity of the noise that TANSs produce increases in these sectors.
- Some switching process turn on/off (modulate) TANSs during thermal cycles (consecutive LFNS experiments). This can be observed on the noise map in Fig. 6c. TANSs with activation energy 0.52 eV and 0.26 eV switch on/off at temperatures 270 K and 180 K, respectively. Most likely origin of the switching process that change the intensity of the corresponding noise and sometimes also activation energy of TANS [18] is a redistribution of local currents driven by relaxation of mechanical stress. It appears in TFRs due to the mismatch of the thermal expansion coefficients of the materials contained in resistive film, conductive terminations and the substrate [18].
- The number of TANSs, and magnitude of the signal they produce, decreases with decreasing sheet resistivity. Decreasing firing temperature makes TANSs less intensive and frequent and annealing does not remove TANSs [18].

5.2. Integral measure of noise

Since noise maps are sample-dependent, also temperature dependencies of power of resistance fluctuations, $\langle \delta R^2 \rangle(T)$, are different, even for TFRs taken from the same series. On the contrary, integral measure of noise [15]:

$$s_T \equiv \frac{1}{T_2 - T_1} \int_{T_1}^{T_2} \int_{f_l}^{f_u} S_R(f, T) df dT, \quad (1)$$

averages temperature and frequency variations and makes possible quantitative comparison of noise properties of different materials [15–17]. In fact, the inner integral in Eq. (1) is the total power, $\langle \delta R^2 \rangle$, of resistance fluctuations in frequency band $f_l - f_u$, which is then averaged over temperature range $T_1 - T_2$. In calculation of s_T, the frequency band from 10 to 100 Hz, and temperature range from 77 K to 300 K have been taken [15–17].

The noise of the whole TFR, (measured on terminations 7–7) has been split up into two components. Bulk and contact noise components have been extracted from linear dependence of s_T on the sector volume [15], which is expected for spatially uncorrelated noise sources. The above approach enables evaluation of (i) dimension-independent bulk noise intensity C_{bulk}, used for comparison of noise properties of different materials, and (ii) contact-geometry-independent parameter C_{int}, which value corresponds to the hypothetical length of the resistive film having the noise equal the interface noise [15–17].

5.3. Materials compatibility

Three parameters are taken into account when comparing materials for TFRs fabrication [15]: (i) size effect *SE*, which reflects influence of contacts on TFRs resistance, (ii) interface quality described by C_{int}, (iii) *NR* parameter, describing non-stationarity of the noise measured for the whole TFR. The spread Δs_T of s_T values in consecutive LFNS experiments, is mostly induced by non-stationarity of interface noise. *NR* parameter, defined as $NR \equiv \max \Delta s_T / \langle s_T \rangle$, relates to changes in microstructure, what might result in device damage. Hence, it should be the key parameter in high-reliability applications. Although, C_{int} and *SE* are non-critical performance parameters, their large values might (i) lead to distortion of nominal values of noise and/or resistance, and (ii) predict long-term drift [25] of resistance resulting in malfunctioning of the device or the overall electrical circuit [26,27]. Hence, compatible systems of pastes for TFRs production should be described by low values of *SE* and C_{int}. However, it should be noted that satisfactory values of parameter $SE \approx 1$ have been found for nearly all examined samples. It thus occurs that only the values of C_{int}, derived from noise measurements, give the information on the quality of interface in TFRs made of various combinations of resistive and conductive pastes. Typical values of C_{int} were ~1 mm, but for lab-made TFRs of RuO_2 and PtAg contacts, C_{int} reached the value of 80 mm.

Thorough studies performed on TFRs [4] [15–18] lead to the following conclusions concerning compatibility of materials used for TFRs fabrication:

- RuO_2-glass based resistive pastes form well behaved contacts with Au-based conductive pastes. Metech 3612 paste is worth to recommend since contact made of it features low size effect, low contact noise and is resistant to switching phenomena. On the other hand, Ag-based conductive pastes should not be used in conjunction with RuO_2-glass based resistive pastes.
- $Bi_2Ru_2O_7$-based resistive pastes make good contacts with Au-based conductive pastes. PdAg-based pastes are acceptable, however they form contact subjected to switching phenomena especially in TFRs of high resistivity. PtAu-based conductive pastes form bad contacts due to the glass conflict.
- Pb/Cd-free RuO_2- and $CaRuO_3/RuO_2$-based resistive pastes form well behaved contacts with different conductive pastes (Ag, Ag–AgPt–Pd, AgPd). However Ag–AgPt–Pd contacts, make $CaRuO_3/RuO_2$ TFRs subject to spectra switching.
- Optimized systems of materials for LTCC work well (DP2041/6146/951), especially in TFRs of high resistivity.

5.4. Noise of resistive films

It has been proved by means of theoretical considerations and verified experimentally, that bulk noise of TFRs is proportional to resistivity ρ, $C_{bulk} = K'\rho$, provided resistivity is changed by the content of conductive constituent of the resistive paste [28–30]. This is illustrated in Fig. 7, where various experimental data are plotted as

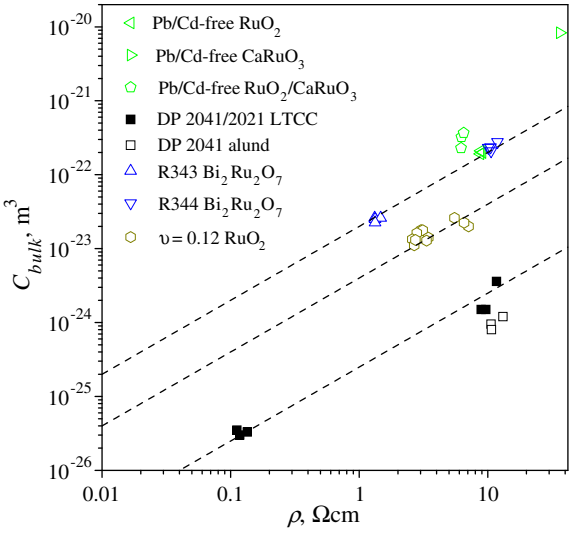

Fig. 7. C_{bulk} parameter plotted vs. resistivity for various materials used for TFRs preparation. Lines are plots of the relation $C_{bulk} = K'\rho$, for different values of K'.

C_{bulk} vs. resistivity [15–17]. Pb/Cd-free $CaRuO_3$-based sample (Fig. 7) had very poor noise properties [16]. Much better are resistors made of newly prepared resistive $RuO_2/CaRuO_3$-based paste, which have the values of C_{bulk} [17] close to that of Pb/Cd-free RuO_2-based films [16] and old-fashioned Pb-containing $BiRu_2O_7$-based films [15]. Even less noisier are Pb-containing RuO_2 films, especially that prepared by the use of LTCC technique [15]. Main reason for increasing noise in Pb/Cd-free RuO_2 films when comparing to Pb-containing RuO_2 films is the difference in grain size, which in studied Pb/Cd-free RuO_2 resistive film was 1 μm while in Pb-containing RuO_2 films it was 10 nm. It has been shown and confirmed experimentally that increase in the grain size results in both larger resistivity and bulk noise [28–32].

Parameter C_{bulk} may be considered as a quality indicator of the resistive film, and should be taken into account when selecting materials for the production of TFRs for low-noise applications, e.g. for temperature sensing in cryogenics. It is also recommended to use C_{bulk} for the comparison of noise properties of different resistive materials, including layered materials for which the relation $C_{us} = KR_{sq}$, where $C_{us} = C_{bulk}/d$ and $R_{sq} = \rho/d$, was found [33]. Let us note, that the ratio K', which enables to compare noise properties of materials of different thicknesses, is generalization of the parameter K, which was originally introduced for the layered materials. Parameters K' and K are equivalent and they are considered to be figure of merit for the $1/f$ noise component. Hence, coefficients $K = 5 \times 10^{-13}$ μm²/Ω found in [33] for Au, poly-Si and poly-SiGe layers and $K' = 2.5 \times 10^{-11}$ μm²/Ω for LTCC TFRs, 4×10^{-10} μm²/Ω for RuO_2 films, 2×10^{-9} μm²/Ω for $Bi_2Ru_2O_7$, $K' = 2 \times 10^{-8}$ μm²/Ω for $CaRuO_3$ films derived from data in Fig. 7, can be directly compared. It occurred that films studied in this work are from 2 to 4 orders of magnitude noisier than the layers examined in [33]. Of some interest can also be comparison with polymer TFRs [34]. For the latter, in contradiction with the above, power-law dependence $C_{bulk} \sim (R_{sq})^{\eta}$ was found, with $\eta = 1.12$, $\eta = 1.18$, and $\eta = 0.76$, for resistors made of medium structured carbon black (MSCB), mixture of MSCB and graphite, and high structured carbon black (HSCB), respectively. This is not surprising, as polymer TFRs, in general, contain less content of conducting constituent and thus are more inhomogeneous so that percolation influences C_{bulk} vs. R_{sq} relation much more [34]. Anyway, direct comparison of C_{bulk} values is still possible. Fitting the data from [34] by the relation $C_{bulk} \sim (R_{sq})^{\eta}$, with $\eta = 1$, the values $K' = 4.3 \times 10^{-11}$ μm²/Ω, 4×10^{-8} μm²/Ω, and 2.7×10^{-11} μm²/Ω have been obtained for MSCB, mixture of MSCB and graphite, and HSCB, respectively. These values of K' are in the range obtained for data presented in Fig. 7.

6. Summary

Excess noise in TFRs is originated from resistance fluctuations, induced by mobility fluctuations. In general, there are two noise components: $1/f$ noise and Lorentzian noise. The latter are visible on noise maps as the streaks. Noise maps obtained by the use of low-frequency noise spectroscopy in temperature range from 4 K to 300 K revealed phenomena that take place in TFRs and could not be observed in single spectrum nor at smooth $R(T)$ curves. TANSs have been detected in all but LTCC TFRs. The population of TANSs is larger in parts of the resistive film adjacent to the interface, indicating that the quality of resistive-to-conductive interface is the key issue in TFRs for low-noise and high-reliability applications. Furthermore, since TANSs might be the origin of spectra switching, special care has to take while selecting materials for production of low-noise and reliable TFRs, especially for low-temperature applications, where noise increases. Luckily, the population of TANSs is large only in commercial temperature range, and no TANSs were detected for $T < 15$ K.

Integral measure of noise occurred to be useful in obtaining noise parameters C_{int}, C_{bulk}, and NR, which have been then used in formulation of materials compatibility criteria. Systems of compatible materials have been described, what might be helpful for further improvement of thick-film technology, especially for manufacturing low-noise, stable and reliable TFRs.

Although noise in studied Pb/Cd-free RuO_2- and $RuO_2/CaRuO_3$-based TFRs is still larger than in their Pb-containing predecessors, $CaRuO_3$ is considered as a more promising candidate for the conducting phase of modern resistive pastes, because it better works with Pb/Cd-free glasses than, for example RuO_2 [35].

Acknowledgments

The work has been supported in part by Grant No. N N515 341836 from Polish Ministry of Science and Higher Education, and Rzeszow University Project No. U7371/DS.

References

[1] Willekers RW, Mathu F, Meijer HC, Postma H. Thick-film thermometers with predictable R-T characteristics and very low magnetoresistance below 1 K. Cryogenics 1990;30:351–5.
[2] Bat'ko I, Flachbart K, Somora M, Vanický D. Design of RuO_2-based thermometers for the millikelvin temperature range. Cryogenics 1995;35:105–8.
[3] Watanabe M, Morishita M, Ootuka Y. Magnetoresistance of RuO_2-based resistance thermometers below 0.3 K. Cryogenics 2001;41:143–8.
[4] Kolek A, Stadler AW, Ptak P, Zawiślak Z, Mleczko K, Szałański P, et al. Low-frequency $1/f$ noise of RuO_2-glass thick resistive films. J Appl Phys 2007;102:103718.
[5] Ptak P, Kolek A, Zawiślak Z, Stadler AW, Mleczko K. Noise resolution of RuO_2-based resistance thermometers. Rev Sci Instrum 2005;76:014901.
[6] Pike GE, Seager CH. Electrical properties and conduction mechanisms of Ru-based thick-film (cermet) resistors. J Appl Phys 1977;48:5152–69.
[7] Sheng P, Sichel EK, Gittleman JI. Fluctuation-induced tunneling conduction in carbon–polyvinylchloride composites. Phys Rev Lett 1978;40:1197–200.
[8] Flachbart K, Pavlik V, Tomasovicova N, Adkins CJ, Somora M, Lieb J, et al. RuO_2-based low temperature sensors with "tuned" resistivity dependencies. Phys Stat Solidi (b) 1998;205:399–404.
[9] Roman J, Pavlik V, Flachbart K, Adkins CJ, Lieb J. Electronic transport in RuO_2-based thick-film resistors at low temperatures. J Low Temp Phys 1997;108:373–82.
[10] Hill R. Electrical transport in thick-film resistors. Electrocomp Sci Technol 1980;6:141–5.
[11] Prudenziati M. On the temperature coefficient of resistivity in thick-film resistors and the percolation model. Alta Frequenza 1979;XLVI 147:E-287–8.
[12] Affronte M, Campani M, Piccinini S, Tamborin M, Morten B, Prudenziati M, et al. Low temperature electronic transport in RuO_2-based cermet resistors. J Low Temp Phys 1997;109:461–75.
[13] Vest RW. Conduction mechanisms in thick-film microcircuits. Final Technical Report. ARPA Order Number 1642:1975.
[14] Affronte M, Campani M, Morten B, Prudenziati M, Laborde O. Magnetoresistance of RuO_2-based thick-film resistors. J Low Temp Phys 1998;112:355–71.
[15] Mleczko K, Zawiślak Z, Stadler AW, Kolek A, Dziedzic A, Cichosz J. Evaluation of conductive-to-resistive layers interaction in thick-film resistors. Microelectron Reliab 2008;48:881–5.
[16] Stadler AW, Kolek A, Zawiślak Z, Mleczko K, Jakubowska M, Kiełbasiński KR, et al. Noise properties of Pb/Cd-free thick-film resistors. J Phys D: Appl Phys 2010;43:265401.
[17] Stadler AW, Zawiślak Z, Kolek A, Kiełbasiński KR, Jakubowska M. Further improvement of Pb/Cd-free $CaRuO_3$ thick-film resistors. IMAPS-CPMT Poland Conference, Wrocław, 2010.
[18] Kolek A, Stadler AW, Zawiślak Z, Mleczko K, Dziedzic A. Noise and switching phenomena in thick-film resistors. J Phys D: Appl Phys 2008;41:025303.
[19] For a review of LTCC technology see e.g. Kolek A, Ptak P, Dziedzic A. Noise characteristics of resistors buried in low-temperature co-fired ceramics. J Phys D: Appl Phys 2003;36:1009–1017.
[20] Stadler AW. Noise signal analyzer for multi-terminal devices. In:.Proc 31st int. conf. of IMAPS Poland chapter (Poland, Rzeszów – Krasiczyn) 2007. p. 413–6.
[21] Stadler AW, Kolek A. Numerical simulations of low-frequency noise in RuO_2-glass films. Proc SPIE 2007;6600. 66000Q1–10.
[22] Skrbek L, Stehno J, Sebek J. Resistance relaxation in carbon and RuO_2 based thermometers. J Low Temp Phys 1996;103:209–38.
[23] Black RD, Restle PJ, Weissman MB. Hall effect, anisotropy, and temperature-dependence measurements of $1/f$ noise in silicon on sapphire. Phys Rev B 1983;28:1935–43.

[24] Pellegrini B, Saletti R, Terreni P, Prudenziati M. $1/f^{\gamma}$ noise in thick-film resistors as an effect of tunnel and thermally activated emissions, from measures vs. frequency and temperature. Phys Rev B 1983;27:1233–43.
[25] Rocak D, Belavic D, Hrovat M, Sikula J, Koktavy B, Pavelka J, et al. Low-frequency noise of thick-film resistors as quality and reliability indicator. Microelectron Reliab 2001;41:531–42.
[26] Jevtić MM. Noise as a diagnostic and prediction tool in reliability physics. Microelectron Reliab 1995;35:455–77.
[27] Jevtić MM, Mrak I, Stanimirović Z. Thick-film quality indictor based on noise index measurements. Microelecron Reliab 1999;30:1255–9.
[28] Vandamme LKJ. Criteria of low-noise thick-film resistors. Electrocomp Sci Technol 1977;4:171–7.
[29] Wolf M, Müller F, Hemschik H. Comment on the dependence of $R_{\square}$ and current noise on grain size in thick-film resistors—TFR's. Active Passive Elec Comp 1985;12:59–61.
[30] Müller F, Wolf M. Dependence of the sheet resistivity and current noise behaviour of the grain size and volume fraction of conducting material in thick-film resistors experiments. Active Passive Elec Comp 1988;13:1–6.
[31] Rao YS. Studies on electrical properties of polymer thick-film resistors. Microelectron Int 2007;24/1:8–14.
[32] Tamborin M, Piccinini S, Prudenziati M, Morten B. Piezoresistive properties of RuO_2-based thick-film resistors: the effect of RuO_2 grain size. Sens Actuat 1997;A 58:159–64.
[33] Vandamme LKJ, Casier HJ. The $1/f$ noise vs. sheet resistance in poly-Si is similar to poly-SiGe resistors and Au-layers. In:.Proceedings of 34th European solid-state device research conf. Leuven, Belgium; 21–23 September, 2004. p. 21–3.
[34] Dziedzic A, Kolek A. $1/f$ noise in polymer thick-film resistors. J Phys D Appl Phys 1998;31:2091–7.
[35] Rane S, Prudenziati M, Morten B, Golonka L, Dziedzic A. Structural and electrical properties of perovskite ruthenate-based lead-free thick-film resistors on alumina and LTCC. J Mater Sci Mater in Electron 2005;16: 687–91.